Catalysis Today 187 (2012) 97–103

Contents lists available at SciVerse ScienceDirect

Catalysis Today

journal homepage: www.elsevier.com/locate/cattod

New inorganic–organic hybrid materials based on SBA-15 molecular sieves involved in the quinolines synthesis

Jesús López-Sanz[a], Elena Pérez-Mayoral[a,*], Elena Soriano[b], Marina Sturm[a], Rosa María Martín-Aranda[a], Antonio J. López-Peinado[a], Jiří Čejka[c,d,**]

[a] Departamento de Química Inorgánica y Química Técnica, Facultad de Ciencias, UNED, Paseo Senda del Rey 9, 28040 Madrid, Spain
[b] Laboratorio de Radicales Libres y Química Computacional (IQOG, CSIC), C/Juan de la Cierva 3, 28006 Madrid, Spain
[c] Department of Synthesis and Catalysis, J. Heyrovský Institute of Physical Chemistry, Academy of Sciences of the Czech Republic, v.v.i., Dolejškova 3, 182 23 Prague 8, Czech Republic
[d] King Saud University, P.O. Box 2455, Riyadh 11451, Saudi Arabia

ARTICLE INFO

Article history:
Received 26 July 2011
Received in revised form 1 December 2011
Accepted 9 December 2011
Available online 14 January 2012

Keywords:
Mesoporous molecular sieve
Heterogeneous catalysis
Quinolines
SBA-15

ABSTRACT

In this paper we report on the first mesoporous catalyst based on SBA-15 incorporating simultaneously basic and acid functions able to promote the Friedländer reaction between 2-aminoaryl ketones and ethyl acetoacetate leading to quinolines **1** with high yields. From 2-aminobenzophenone (**3a**) it is possible to prepare quinoline **1a** with the highest selectivity (86%) as compared with other mesoporous acidic catalysts. In contrast, the reaction catalyzed by amine-grafted SBA-15 yielded selectively (98%) the corresponding quinolone **2a** in accordance with our previous results. Experimental results have been justified by theoretical calculations as function of the stability of reaction intermediate species, which could be involved in the process.

1. Introduction

Development of new materials, among them those based on mesoporous structures, involved in green chemical processes is a current and challenging topic of fundamental importance in the design of novel and more efficient environmental friendly catalysts [1]. Discovery of silica-based mesoporous materials attracted the attention of many researchers since the development of these types of molecular sieves contributed to extending the range from microporous and ordered zeolitic materials into the mesoporous regime [2]. However, these ordered mesoporous materials show neutral silica frameworks considerably limiting their applications in catalysis. In order to transform those in supports potentially useful as catalysts, it is necessary to introduce catalytic functions often by incorporation of organic functional moieties bound into their walls or by deposition of active species on their inner surface or to use layered zeolites with large accessible external surfaces [3]. The main advantages of ordered mesoporous solids in catalysis are (i) relatively large pores as compared with microporous materials like zeolites, facilitating the reactants/products diffusion, and (ii) very high surface areas allowing the introduction of high concentrations of active sites. Both these features contribute to increase overall reaction rates of catalytic processes catalyzed by mesoporous molecular sieves.

Recently, we reported on the synthesis of quinolines **1**/quinolin-2(1*H*)-ones **2** via Friedländer reaction (Scheme 1) by condensation of 2-aminoaryl ketones **3** with ethyl acetoacetate **4**, in toluene at 373 K, promoted by acid or basic mesoporous catalysts such as amino grafted MCM-41, Al(SBA-15) and also zeolites [4]. While the condensation catalyzed by acid catalysts yielded mixtures of corresponding quinolin-2(1*H*)-ones **2** and quinolines **1**, dramatic selectivity changes were observed when using amino grafted MCM-41 materials. Quinolones **2** were isolated with quantitative yield and total selectivity.

Friedländer condensation is considered an economic atom reaction consisting of a double condensation between 2-aminoaryl carbonyl compounds with other carbonyl compounds, exhibiting enolizable hydrogens. It is useful and the simplest synthetic approach for the preparation of substituted quinolines [5]. These nitrogen heterocycles represent important substrates in medicine, food, catalyst, dye, materials, refineries and electronics [6].

From a green chemistry point of view, only a few heterogeneous catalysts have been reported to be active in Friedländer reaction,

---

[*] Corresponding author. Tel.: +34 91 398 9047; fax: +34 91 398 6697.
[**] Corresponding author at: Department of Synthesis and Catalysis, J. Heyrovský Institute of Physical Chemistry, Academy of Sciences of the Czech Republic, v.v.i., Dolejškova 3, 182 23 Prague 8, Czech Republic. Tel.: +420 26605 3795; fax: +420 28658 2307.
E-mail addresses: eperez@ccia.uned.es (E. Pérez-Mayoral), jiri.cejka@jh-inst.cas.cz (J. Čejka).

0920-5861/$ – see front matter © 2011 Elsevier B.V. All rights reserved.
doi:10.1016/j.cattod.2011.12.015

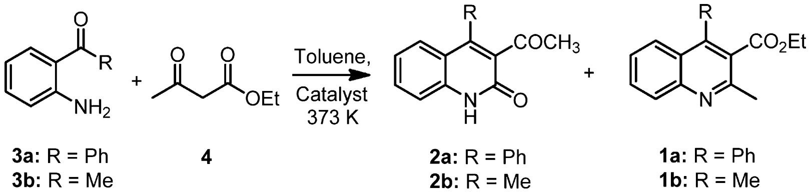

Scheme 1. Friedländer reaction of 2-aminoaryl ketones and ethyl acetoacetate.

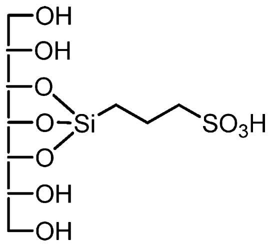

Fig. 1. Mesoporous materials named SBA-15/S.

namely Al_2O_3 [7], H_2SO_4/SiO_2 [8–10], $NaHSO_4/SiO_2$ [11,12], $HClO_4/SiO_2$ [13], silica gel-supported phosphomolybdic acid [14], $KAl(SO_4)_2{\cdot}12H_2O/SiO_2$ [15], sulfonated cellulose [16] and silica-propylsulfonic acid [17]. In this sense and contributing to the development of new and efficient mesoporous catalysts for this transformation, we recently communicated on the first example of Friedländer reaction promoted by a Metal-Organic-Framework, $[Cu_3(BTC)_2]$ showing superior activity [18].

Our present interest is focused on the synthesis and characterization of new inorganic–organic hybrid mesoporous material based on SBA-15 showing bifunctional organic linkers simultaneously incorporating basic and acid sites, more specifically, amine groups and sulfonic acids. In this paper, we also report on its catalytic performance in the Friedländer reaction between 2-aminoaryl ketones and ethyl acetoacetate, useful synthetic methodology for the preparation of quinolines.

2. Experimental

2.1. Synthesis of the catalysts

SBA-15 was synthesized according to the methodology previously reported [19].

2.1.1. Synthesis of SBA-15/S

SBA-15/S was prepared starting from SBA-15 support by reaction with 3-(triethoxysilyl)propane-1-thiol and subsequent oxidation of the thiol group with hydrogen peroxide following the experimental protocol reported by Pérez-Pariente et al. [20] (Fig. 1).

2.1.2. Synthesis of amino-grafted SBA-15, SBA-15/AP

Amino-grafted SBA-15 materials were synthesized according to the experimental procedure reported in Ref. [21] starting from SBA-15 support and using trialkoxysilylpropylamine. In more detail, to a suspension of dried SBA-15 (2 g) in toluene (35 mL), (3-aminopropyl)trimethoxysilane (6.65 mmol, molar excess) was added and the mixture was stirred for 5 h at room temperature (296 K). Then, toluene was filtered off and the modified SBA-15 was washed out three times with toluene (20 mL). Finally, the SBA-15/AP was dried in vacuum at room temperature (Scheme 2).

2.1.3. Synthesis of SBA-15/APS

SBA-15/APS was prepared from SBA-15/AP by reaction with γ-sultone (Scheme 2). Then, to a suspension of SBA-15/AP (0.5 g) in toluene (20 mL), γ-sultone (5 mmol) was added and the reaction mixture was stirred for 24 h at 363 K. After cooling to ambient temperature, the modified SBA-15 was filtered off and washed out three times with toluene (20 mL). Finally, SBA-15/APS was dried in vacuum at room temperature (Scheme 2).

2.2. Characterization of the catalyst

2.2.1. Nitrogen adsorption

Adsorption isotherms of nitrogen at 77 K on molecular sieves under study were recorded using a static volumetric apparatus ASAP 2020 (Micromeritics). In order to attain a sufficient accuracy in the accumulation of the adsorption data, this instrument is equipped with pressure transducers covering the 133 Pa and 133 kPa ranges. Before each sorption measurement the samples were outgassed at 383–393 K overnight until the residual pressure was lower than 0.7 Pa. Table 1 lists some characterization data of the catalysts under study.

2.2.2. Thermal stability

Thermal stability of the solids based on SBA-15 structure was investigated by TG experiments using a TA Instrument SDT Q600.

2.2.3. X-ray diffraction (XRD)

The structure of all synthesized materials was confirmed by X-ray powder diffraction with a Seifert C-3000 diffractometer with filtered Cu Kα radiation in the Bragg-Brentano geometry operating at 40 kV and 30 mA, over powder samples. X-ray powder diffraction patterns of all mesoporous materials provided clear evidence of their hexagonal structure and phase purity of samples under investigation.

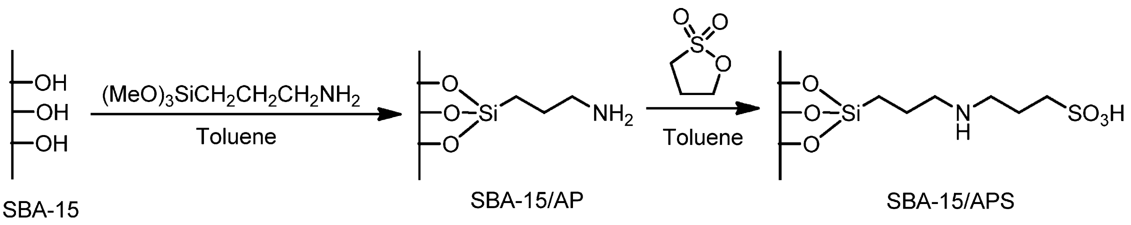

Scheme 2. Preparation of SBA-15/APS.

Table 1
Characterization data of the mesoporous materials based on SBA-15.

Catalyst	S_{BET} (m^2/g)	D^a (Å)	V^a (m^3/g)	C^b (mmol/g)	N^b (mmol/g)	S^b (mmol/g)
SBA-15	834	56	0.97	–	–	–
SBA-15/S	556	55	0.78	2.18	–	0.50
SBA-15/AP	292	55	0.49	5.71	1.69	–
SBA-15/APS	254	53	0.48	8.89	1.40	1.42

S_{BET}, BET surface area. *D* and *V* diameter and volumen of the pores, respectively.

[a] Determined by BJH method.

[b] Determined by elemental analysis.

2.3. Catalytic activity

2.3.1. General

NMR spectra were recorded with a Bruker AVANCE DPX-300 (300 MHz for ^{1}H). ^{1}H chemical shifts (δ) in DMSO-d_6 are given from internal tetramethylsilane.

TLC chromatography was performed on DC-Aulofolien/Kieselgel 60 F245 (Merck). All reagents and solvents were purchased from Aldrich and Alfa-Aesar.

2.3.2. Experimental procedure

Prior to the reaction catalysts were activated at 363 K for 5 h.

In a typical procedure, the catalyst (25 mg) was added to a solution of the corresponding 2-aminoaryl ketone **3** (1 mmol) and ethyl acetoacetate **4** (5 mmol), at 363 K, and the reaction mixture was stirred during the time shown in Table 2. After cooling, DMF (2 mL) was added to the reaction crude and the catalyst was filtered off. Subsequently, DMF was evaporated in vacuo.

Reactions were followed by TLC using mixtures of hexane/AcOEt or CH_2Cl_2/EtOH as eluents.

Reaction products were characterized by ^{1}H NMR. Spectroscopic data of the synthesized products are according to those previously reported [4].

2.4. Theoretical calculations

All calculations were performed with the Gaussian 03 suite of programs [22]. Geometry optimizations were performed using the B3LYP [23] density functional method in conjunction with the 6-311G(3d,2d) basis set. They were verified to have all real harmonic frequencies by frequency calculations, which also provided thermal corrections to enthalpy.

The electron population analysis was performed on the optimized structures of the reactants **3a**,**b** with the Atomic Polar Tensor (APT) model [24] because it is relatively independent of the level of theory.

Each isomer of the presumed key intermediate **6** (see Scheme 3) was subjected to conformational searching at the B3LYP/6-311G(3d,2p) level in order to identify the lowest-energy isomer. The conformational preferences of linear model molecules were examined through the multidimensional conformational analysis

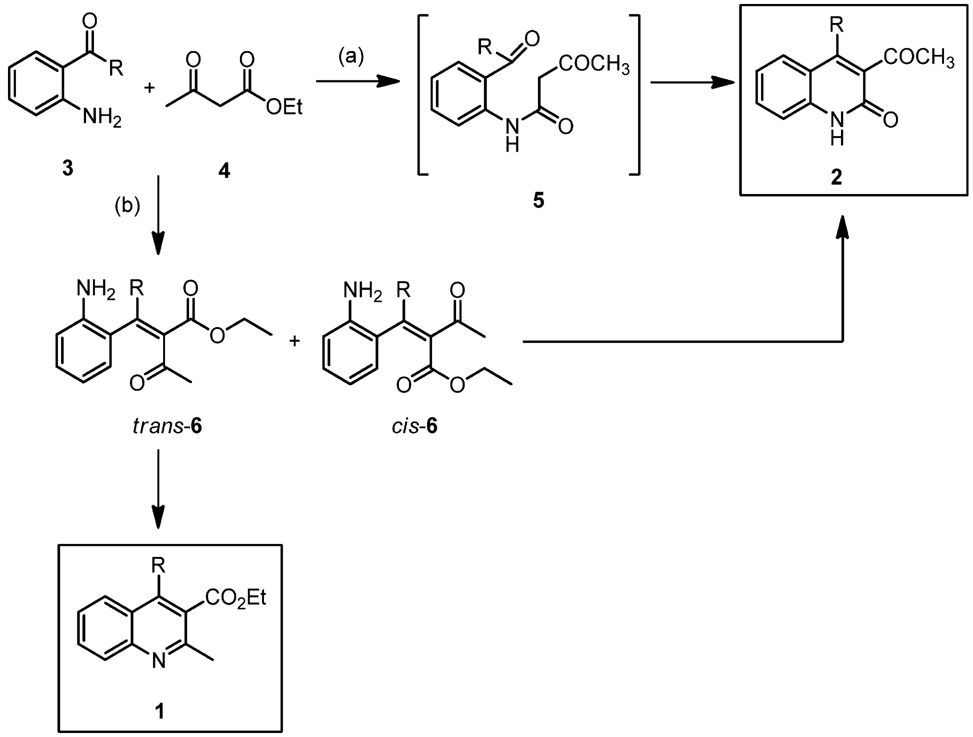

Scheme 3. Pathways for the synthesis of quinolines **1**/quinolones **2** by using acid and basic mesoporous catalysts.

Table 2
Friedländer condensation of 2-aminobenzophenone (**3a**) and ethyl acetoacetate (**4**) at 363 K.

Catalyst	Time (h)	*Y* of **1a** (%)	*S* to **1a**	*Y* of **2a** (%)	*S* to **2a**	TON	TOF (h^{-1})
SBA-15/APS	3	86	86	14	14	2857	952
SBA-15/AP	3	3	9	63	95	1571	524
	6	2	2	96	98	2333	389
SBA-15/S	3	67	73	25	27	10454	3484

Y, yield; *S*, selectivity.

(MDCA) strategy: all the minima that can be anticipated considering that each flexible dihedral angle is expected to have three minima, were constructed by systematic rotation of the single bonds and subsequently optimized.

3. Results and discussion

3.1. Synthesis and characterization of the mesoporous materials

In this work we have synthesized three different mesoporous materials incorporating basic or acid functions or both of those. At first, we prepared SBA-15/S containing sulfonic acids as active catalytic centres according to Ref. [20] (Fig. 1). Amino-grafted SBA-15/AP was synthesized as starting support for the synthesis of SBA-15/APS, the last one incorporating both secondary amine and sulfonic acid groups (Scheme 2).

Specific surface areas of all materials were determined from nitrogen adsorption isotherms being in a range of 556–254 m^2/g; a decrease in the specific surface area was observed depending on the function sizes as expected. Then, SBA-15/APS was the mesoporous material showing the lowest surface area. Diameter and volume of the pores were in the ranges of 56–53 Å and 0.78–0.48 cm^3/g, respectively (Table 1).

Chemical composition of the solids was investigated by elemental analysis. Slightly higher concentration of S (1.419 mmol/g) in SBA-15/APS compared with the N content (1.400 mmol/g) suggests a lower concentration of sulfonic acids, 0.019 mmol/g, distributed on the surface of the catalyst; therefore, the structure of SBA-15/APS could be represented as shown in Fig. 2.

Thermal stability of the catalysts was investigated by thermogravimetry (TG), all of them being stable in a temperature range from room temperature to approximately 473 K. It is important to note that the thiol and sulfonic acid groups located in the inner surface on SBA-15/S decompose at different temperatures in accordance with the results reported by Margolese et al. [25] and Trejda et al. [26]. In this sense, considering the TG measurements and the composition determined by elemental analysis we calculated the active site concentration referred to sulfonic acid centres in SBA-15/S. The concentrations of thiol and sulfonic acid species in SBA-15/S were approximately 0.15 and 0.35 mmol/g, respectively. Therefore, post-synthesis activation of SBA-15 by treatment with (triethoxysilyl)propane-1-thiol and subsequent oxidation of the thiol groups using an excess of hydrogen peroxide provided the mesoporous solid SBA-15/S containing higher concentration of sulfonic acids.

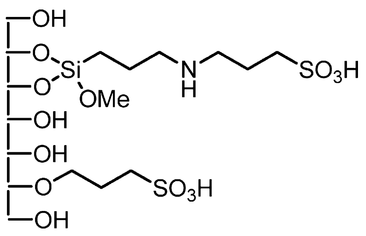

Fig. 2. Possible structure of SBA-15/APS.

XRD patterns for all SBA-15 molecular sieves reported here showed analogs profiles with well-resolved diffraction lines at low angles evidencing the hexagonal structure of SBA-15 materials (Fig. 3).

3.2. Catalytic performance

Molecular sieves described above were tested as catalysts in the Friedländer condensation using differently substituted 2-aminoaryl ketones **3** and ethyl acetoacetate **4** under solvent-free conditions. The reaction between 2-aminobenzophenone (**3a**) and ethyl acetoacetate (**4**), catalyzed by SBA-15/APS, at 363 K, yielded the quinoline **1a** in 62% with high selectivity (84%) after 1 h of reaction time (Scheme 1 and Fig. 4). Note that the reaction was completed after 3 h affording mixtures of quinoline **1a** and quinolone **2a** in 86 and 14%, respectively (Table 2 and Fig. 4). In contrast, when we carried out the reaction over SBA-15/AP for 6 h, the corresponding quinolone **2a** was isolated in 92% almost as unique reaction product. Only traces (<2%) of compound **1a** being obtained. Although the reaction took place in the presence of toluene as a solvent when using amino-grafted MCM-41 [4a] and absence of that catalyzed by SBA-15/AP affording quinolone **2a**, yield of **2a** being notably higher when operating under solvent-free conditions (92%).

Therefore, we report here on two methodologies allowing the selective synthesis of quinoline **1a** or quinolone **2a** from 2-aminobenzophenone (**3a**) and ethyl acetoacetate (**4**) depending on the used catalyst. When using SBA-15/AP, basic catalyst, quinolone **2a** was almost exclusively isolated with high yield whereas in the reaction catalyzed by SBA-15/APS, the selectivity was inverted yielding the corresponding quinoline **1a** with high yields.

In addition, the condensation of **3a** and **4** catalyzed by SBA-15/S gave, after 3 h of the reaction time, mixtures of compounds **1a** and **2a** in 67 and 25%, respectively (Table 2).

Turnover number (TON) and turnover frequency (TOF) are defined as TON = conversion (%) (mmol(substrate))/mmol (catalyst) while TOF = TON/time (h).

Fig. 4 depicts the yield of quinoline **1a** and quinolone **2a** vs. time; note that both compounds, **1a** and **2a**, are formed at the shortest

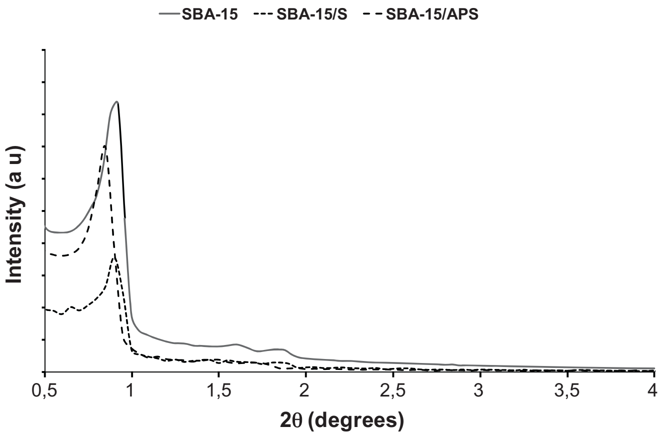

Fig. 3. X-ray diffraction patterns for SBA-15, SBA-15/S and SBA-15/APS.

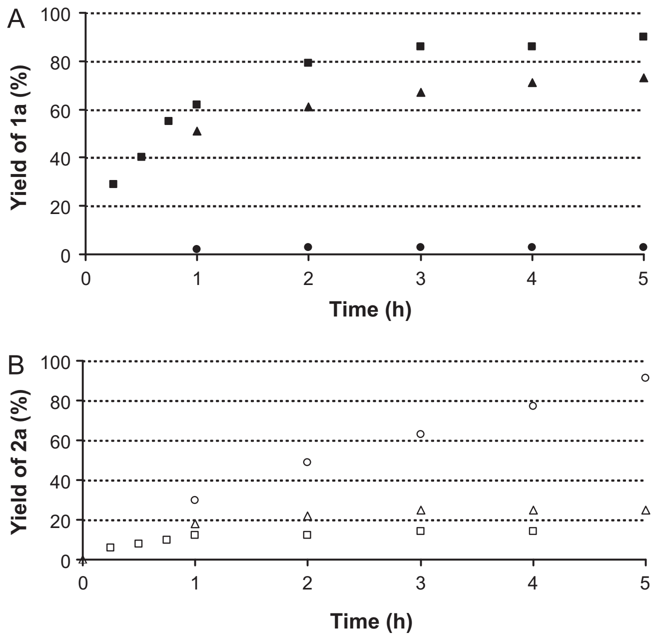

Fig. 4. Friedländer reaction of **3a** and **4** catalyzed by mesoporous silicates; (A) Yield of **1a** vs. time; (■) SBA-15/APS, (▲) SBA-15/S, (●) SBA-15/AP. (B) Yield of **2a** vs. time; (□) SBA-15/APS, (△) SBA-15/S, (○) SBA-15/AP.

reaction times in the reaction catalyzed by SBA-15/APS and SBA-15/S, respectively. However, after 2 h of the reaction, yields of **2a** were approximately 14% and 25% while yield of quinoline **1a** was increased during all studied times.

We also investigated the condensation of 2-aminoacetophenone (**3b**) with **4** over SBA-15/APS as catalyst under solvent-free conditions at 363 K. In this case, mixtures of compounds **1b** (62%) and **2b** (38%) were isolated after 1 h of the reaction time. It is important to note that after only 1 h the reaction was completed but quinoline **1b** was isolated with lower selectivity (62%). Remarkably, after this same time 1 h, quinoline **2a** was obtained with also 62% of yield but improved selectivity (84%) as given in Fig. 1A. Under the same reaction conditions the condensation between **3b** and **4** catalyzed by SBA-15/S led to compounds **1b** and **2b** in 39% and 61% of yield after 4 h of reaction time.

Having in mind all these results, we can affirm that SBA-15/S was found to be the most active catalyst, as demonstrated by the TON and TOF values shown in Table 2, whereas SBA-15/APS was the most selective catalyst in the Friedländer reaction between **3a** and **4** promoting the formation of quinoline **1a** with the highest selectivity.

All these results are in accordance with those previously reported by us when using (Al)SBA-15 or its Cs-analog, in toluene as solvent, yielding in both cases mixtures of the corresponding quinolines **1b** and quinolones **2b** [4a]. Therefore, we can conclude that the Friedländer condensation of **3** with **4** is promoted by mesoporous molecular sieves exhibiting predominantly Lewis acid sites, (Al)SBA-15, or Brønsted acidity, SBA-15/S, leading to mixtures of quinoline **1**/quinolone **2**. Remarkably, when using the hybrid mesoporous molecular sieve, SBA-15/APS, the reaction yielded quinoline **1a** with the highest selectivity.

3.3. Theoretical calculations

In summary, the condensation of **3a** with **4** catalyzed by SBA-15/S afforded quinoline **1a**/quinolone **2a** mixture in a ratio 2.7:1 whereas the process catalyzed by SBA-15/APS led to quinoline **1a** with a higher yield (86%) and selectivity (86%). However, when starting from **3b**, quinoline **1b**/quinolone **2b** mixture in a ratio 3:2 were isolated.

Differences in the 2-aminoaryl ketone **3** behavior might be related to the different structure and stability of the intermediate compounds leading to the corresponding reaction products. In order to explain the experimental results we could consider two different pathways for the reaction depending on the acid-base properties of the catalyst (a) basic and (b) acid or bifunctional mesoporous materials (Scheme 3). While the reaction catalyzed by amino-grafted MCM-41 in toluene [4a], or SBA-15/AP here under solvent-free conditions, takes place probably through the intermediate **5**, which subsequently could provide cyclization affording the corresponding quinolone **1** (Scheme 3, path a), the process catalyzed by acidic mesoporous materials, (Al)SBA-15 or SBA-15/S and SBA-15/APS, could start by aldolic (Knoevenagel) condensation between both carbonyl components in the reactants giving mixtures of the corresponding *cis–trans* isomers **6** (Scheme 3, path b). Then, subsequent cyclization of *cis*-**6** could afford the corresponding quinolone **2** whereas *trans*-**6** yield quinolines **1**.

The formation of the quinolines of type **1** bearing a carboxylic ester and the acidic nature of the catalyst suggest the initial Knoevenagel condensation as operative mechanism. This could be initiated by the activation of the carbonylic oxygen by the acidic sites of the catalyst.

The computational study of the 2-aminoaryl ketones **3a–b** (B3LYP/6-311G(3d,2p)) revealed some relevant properties. The steric effects in **3a** induce the lack of planarity between the ketone moiety and the aromatic groups (the phenyl plane shows a dihedral torsion of 27° and the aminoaryl moiety 39°, Fig. 5). The computed APT charges suggest a more electrophilic carbonyl carbon for **3a** (+1.126) than for **3b** (+0.975). The larger charge separation on the carbonyl group on **3a** than on **3b** would also favor the interaction of the C=O with the catalytic sites thus promoting the reaction. This difference may be due to the inductive effect of the R substituent (Ph vs. Me) and the reduced mesomeric effect in **3a**.

On other hand, preliminary mechanistic studies have revealed some differences in the presumed key intermediates *cis*- and *trans*-**6**. The conformational analysis performed on each isomer has revealed the following. Taking into account the most stable structures for every case, we have observed that all of them involve an intramolecular hydrogen-bond between the amino moiety and a carbonyl group. In addition, the length of this H-bond is shorter for the *trans*-(2.18 Å) than for the *cis*-isomers (2.28–2.39 Å) (NH···O=C—C shorter than NH···O=C—O), mainly for **6a** (Fig. 6).

For **6b**, the non-H bonded carbonylic/carboxylic moiety is coplanar to the olefin, thus minimizing steric repulsions and maximizing interaction (weak H-bond O···H—CH_2—, ~2.2 Å) with the carbonylic substituent in a *s-cis* conformation (C=C—C=O dihedral angle of 13°, for *cis*-**6b**) or in a *s-trans* conformation (dihedral angle of 156°, for *trans*-**6b**). In these situations, it is expected a close energy between both isomers of **6b**.

On the contrary, for **6a**, the phenyl substituent cannot be coplanar with the olefin due to steric and electronic repulsions with the carbonyl/carboxylic ester, also out of the plane. Although stabilizing weak CH–π interactions between the phenyl π-cloud and an H of the methyl group (2.65 Å) are observed for *cis*-**6a** [27], *trans*-**6a** shows the maximum separation between carbonylic oxygen, thus minimizing strong electronic repulsions (Fig. 6).

The computed enthalpies show that the *trans*-isomers of **6a** and **6b** exhibit a lower value than the *cis*-counterparts. However, whereas for **6b** the difference in the enthalpy between both isomers is very small (0.63 kcal/mol), it becomes significant for **6a** (3.09 kcal/mol). This result reveals a thermodynamic preference for

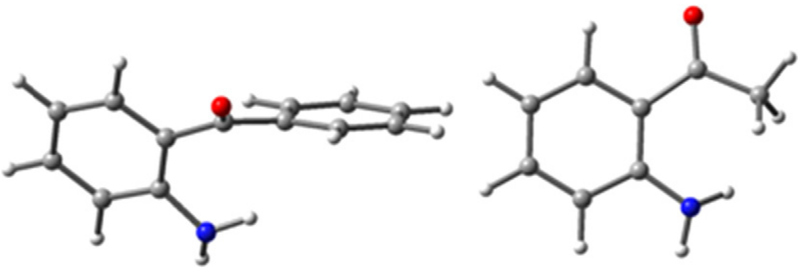

Fig. 5. Optimized structures (B3LYP/6-311G(3d,2p)) of the precursors **3a** (left) and **3b** (right).

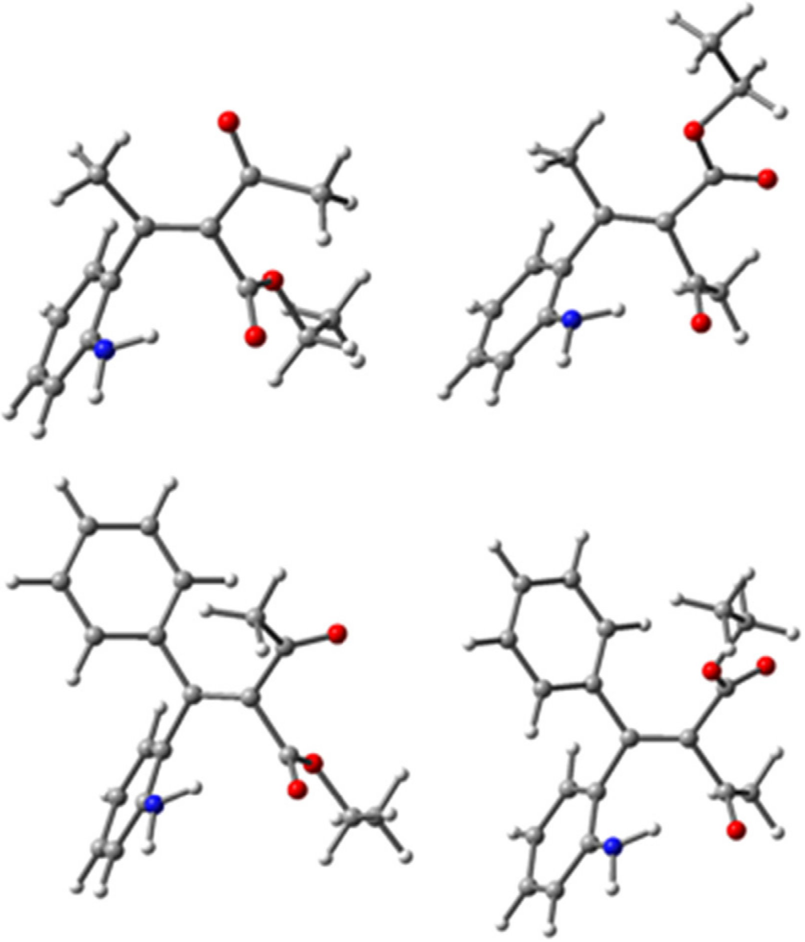

Fig. 6. Optimized structures (B3LYP/6-311G(3d,2p)) of the isomers of **6**: **6a** (bottom), **6b** (top), *cis*-(left), *trans*-(right).

the formation of the key intermediate *trans*-**6a** which would control the evolution of the reaction to the quinoline **1a** and could account for the experimental ratios.

4. Conclusions

In conclusion, mesoporous catalysts here reported were found to be efficient catalysts for the Friedländer condensation between 2-aminoaryl ketones **3** and ethyl acetoacetate **4** providing the corresponding quinolines **1**/quinolones **2**. Acidic mesoporous catalysts, SBA-15/S and SBA-15/APS, yielded mixtures of the corresponding quinolines **1**/quinolones **2** whereas basic catalysts, SBA-15/AP, afforded exclusively quinolone **1b** with excellent yield.

Among the acidic catalysts, SBA-15/S was found to be the most active catalyst, SBA-15/APS being the most selective leading to quinoline **1a**. Moreover, we can drive the condensation towards the formation of quinolone **1a** or quinoline **2a** as function of the used catalyst.

Theoretical calculations on the presumed key intermediates indicate a thermodynamic preference for the formation of the *trans*-isomer **6a** due to the interplay of subtle steric and electronic effects which would drive preferentially to the quinoline product.

Remarkably, the highest reaction selectivity preferentially to quinoline **1a** is achieved when the condensation is catalyzed by SBA-15/APS. Comparing with other acid mesoporous catalysts, it suggests the involvement of sulfonic acids over the catalyst in the reaction, but also probably the amine functions. In this sense, theoretical mechanistic studies are in progress.

Acknowledgements

This work has been supported in part by MICINN (Projects CTQ2009-10478 and CTQ2010-18652). M.S. thanks ERASMUS program (UNED-Ruhr-Universität Bochum) the possibility to investigate in the UNED. The work of J.Č. was supported by the Academy of Sciences of the Czech Republic (KAN 100400701). J.Č. would like to thank Visiting Professor Program, King Saud University, Riyadh, Saudi Arabia.

References

[1] R.M. Martín-Aranda, J. Čejka, Top. Catal. 53 (2010) 141.
[2] A. Taguchi, F. Schüth, Micropor. Mesopor. Mater. 77 (2005) 1.
[3] (a) A. Corma, Chem. Rev. 97 (1997) 2373;
(b) W.J. Roth, J. Čejka, Catal. Sci. Technol. 1 (2011) 43;
(c) W.J. Roth, O.V. Shvets, M. Shamzhy, P. Chlubná, M. Kubů, P. Nachtigall, J. Čejka, J. Am. Chem. Soc. 133 (2011) 6130;
(d) D. Kubička, M. Bejblová, J. Vlk, Top. Catal. 53 (2010) 168;
(e) D. Kubička, P. Šimáček, N. Žilkova, Top. Catal. 52 (2009) 161.
[4] (a) F. Domínguez-Fernández, J. López-Sanz, E. Pérez-Mayoral, D. Bek, R.M. Martín-Aranda, A.J. López-Peinado, J. Čejka, ChemCatChem 1 (2009) 241;
(b) J. López-Sanz, E. Pérez-Mayoral, D. Procházková, R.M. Martín-Aranda, A.J. López-Peinado, Top. Catal. 53 (2010) 1430.
[5] J. Marco-Contelles, E. Pérez-Mayoral, A. Samadi, M.C. Carreiras, E. Soriano, Chem. Rev. 109 (2009) 2652.
[6] S. Madapa, Z. Tusi, S. Batra, Curr. Org. Chem. 12 (2008) 1116.
[7] K. Mogilaiah, K. Vidya, Ind. J. Chem. Sect. B 46B (2007) 1721.
[8] A. Shaabani, E. Soleimani, Z. Badri, Monatsh. Chem. 137 (2006) 181.
[9] M.A. Zolfigol, P. Salehi, M. Shiri, T.F. Rastegar, A. Ghaderi, J. Iran. Chem. Soc. 5 (2008) 490.
[10] B. Das, K. Damodar, N. Chowdhury, R.A. Kumar, J. Mol. Catal. A: Chem. 274 (2007) 148.
[11] M. Dabiri, S.C. Azimi, A. Bazgir, Monatsh. Chem. 138 (2007) 659.
[12] U.V. Desai, S.D. Mitragotri, T.S. Thopate, D.M. Pore, P.P. Wadgaonkar, Arkivoc (2006) 198.
[13] M. Narasimhulu, T.S. Reddy, K.C. Mahesh, P. Prabhakar, Ch.B. Rao, Y. Venkateswarlu, J. Mol. Catal. A 266 (2007) 114.
[14] B. Das, M. Krishnaiah, K. Laxminarayana, D. Nandankumar, Chem. Pharm. Bull. 56 (2008) 1049.
[15] A.A. Mohammadi, J. Azizian, A. Hadadzahmatkesh, M.R. Asghariganjeh, Heterocycles 75 (2008) 947.
[16] A. Shaabani, A. Rahmati, Z. Badri, Catal. Commun. 9 (2008) 13.
[17] D. Garella, A. Barge, D. Upadhyaya, Z. Rodriguez, G. Palmisano, G. Cravotto, Synth. Commun. 40 (2010) 120.
[18] E. Pérez-Mayoral, J. Čejka, ChemCatChem 3 (2011) 157.
[19] A. Zukal, H. Šiklová, J. Čejka, Langmuir 24 (2008) 9837.
[20] I. Díaz, F. Mohino, E. Sastre, J. Pérez-Pariente, Stud. Surf. Sci. Catal. 135 (2001) 1383.
[21] H. Balcar, J. Čejka, J. Sedláček, J. Svoboda, J. Zedník, Z. Bastl, V. Bosáček, J. Vohlídal, J. Mol. Catal. A 203 (2003) 287.
[22] Gaussian 03, Revision E.01, M.J. Frisch, G.W. Trucks, H.B. Schlegel, G.E. Scuseria, M.A. Robb, J.R. Cheeseman, J.A. Montgomery, Jr., T. Vreven, K.N. Kudin, J.C. Burant, J.M. Millam, S.S. Iyengar, J. Tomasi, V. Barone, B. Mennucci, M. Cossi, G. Scalmani, N. Rega, G.A. Petersson, H. Nakatsuji, M. Hada, M. Ehara, K. Toyota, R. Fukuda, J. Hasegawa, M. Ishida, T. Nakajima, Y. Honda, O. Kitao, H. Nakai, M. Klene, X. Li, J.E. Knox, H.P. Hratchian, J.B. Cross, C. Adamo, J. Jaramillo, R. Gomperts, R.E. Stratmann, O. Yazyev, A.J. Austin, R. Cammi, C. Pomelli, J.W. Ochterski, P.Y. Ayala, K. Morokuma, G.A. Voth, P. Salvador, J.J. Dannenberg, V.G. Zakrzewski, S. Dapprich, A.D. Daniels, M.C. Strain, O. Farkas, D.K. Malick, A.D. Rabuck, K. Raghavachari, J.B. Foresman, J.V. Ortiz, Q. Cui, A.G. Baboul, S. Clifford, J. Cioslowski, B.B. Stefanov, G. Liu, A. Liashenko, P. Piskorz, I. Komaromi, R.L. Martin, D.J. Fox, T. Keith, M.A. Al-Laham, C.Y. Peng, A. Nanayakkara, M. Challacombe, P.M.W. Gill, B. Johnson, W. Chen, M.W. Wong, C. Gonzalez, J.A. Pople, Gaussian, Inc., Pittsburgh, PA, 2003.
[23] (a) A.D. Becke, J. Chem. Phys. 98 (1993) 5648;
(b) C. Lee, W. Yang, R.G. Parr, Phys. Rev. B 37 (1988) 785.
[24] J. Cioslowski, J. Am. Chem. Soc. 111 (1989) 8333.
[25] D. Margolese, J.A. Melero, S.C. Christiansen, B.F. Chmelka, G.D. Stucky, Chem. Mater. 12 (2000) 2448.
[26] M. Trejda, K. Stawicka, M. Ziolek, Appl. Catal. B 103 (2011) 404.
[27] O. Takahashi, Y. Kohno, M. Nishio, Chem. Rev. 110 (2010) 6049.